Supplement of Atmos. Chem. Phys., 18, 13531–13545, 2018
https://doi.org/10.5194/acp-18-13531-2018-supplement

Atmospheric Chemistry and Physics
Open Access
EGU

Supplement of

Improving air quality model predictions of organic species using measurement-derived organic gaseous and particle emissions in a petrochemical-dominated region

Craig A. Stroud et al.

Correspondence to: Craig A. Stroud (craig.stroud@canada.ca)

1. Organic Emission Difference Maps between Revised Emissions and Base Case Emissions

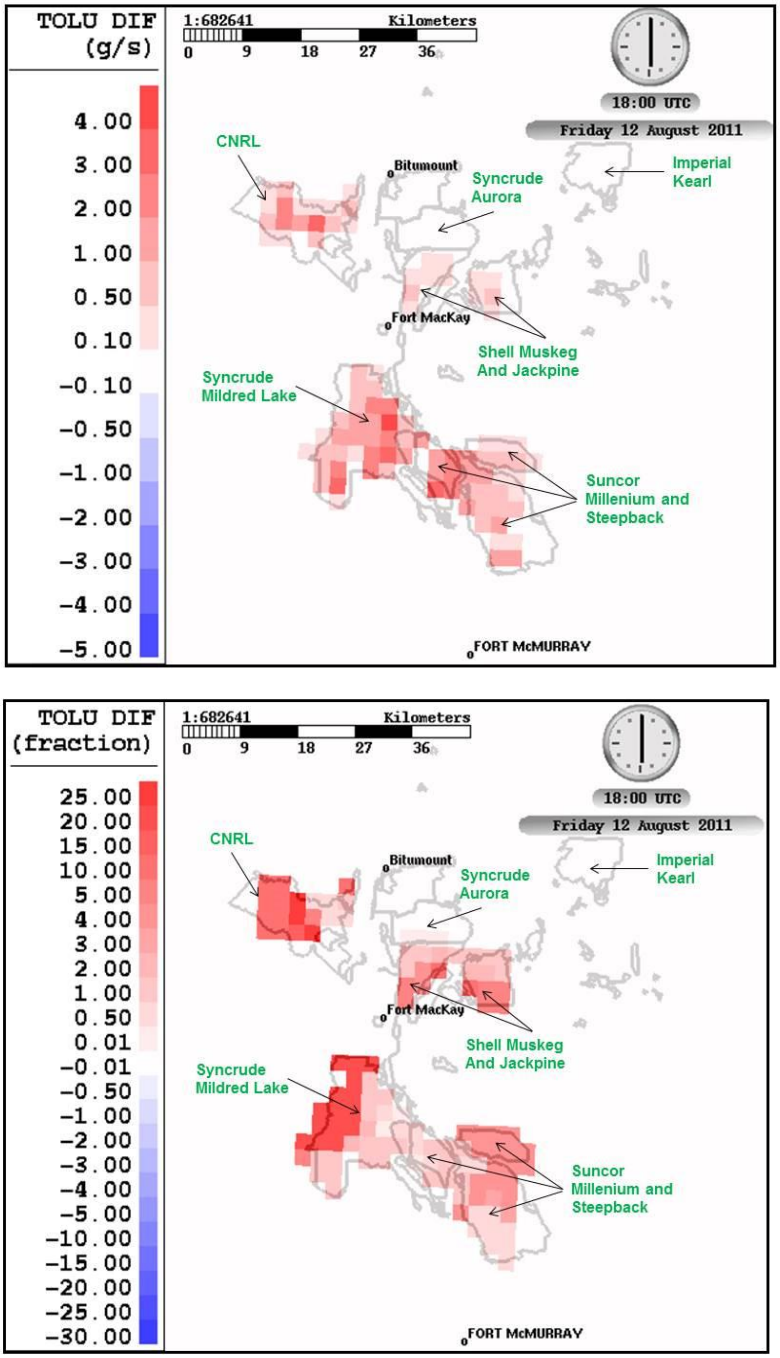

Figure S1. (a) Difference in lumped TOLU emissions (revised-base case) in units of grams/sec for each 2.5-km x 2.5-km grid cell; (b) relative difference calculated as (revised–base)/base.

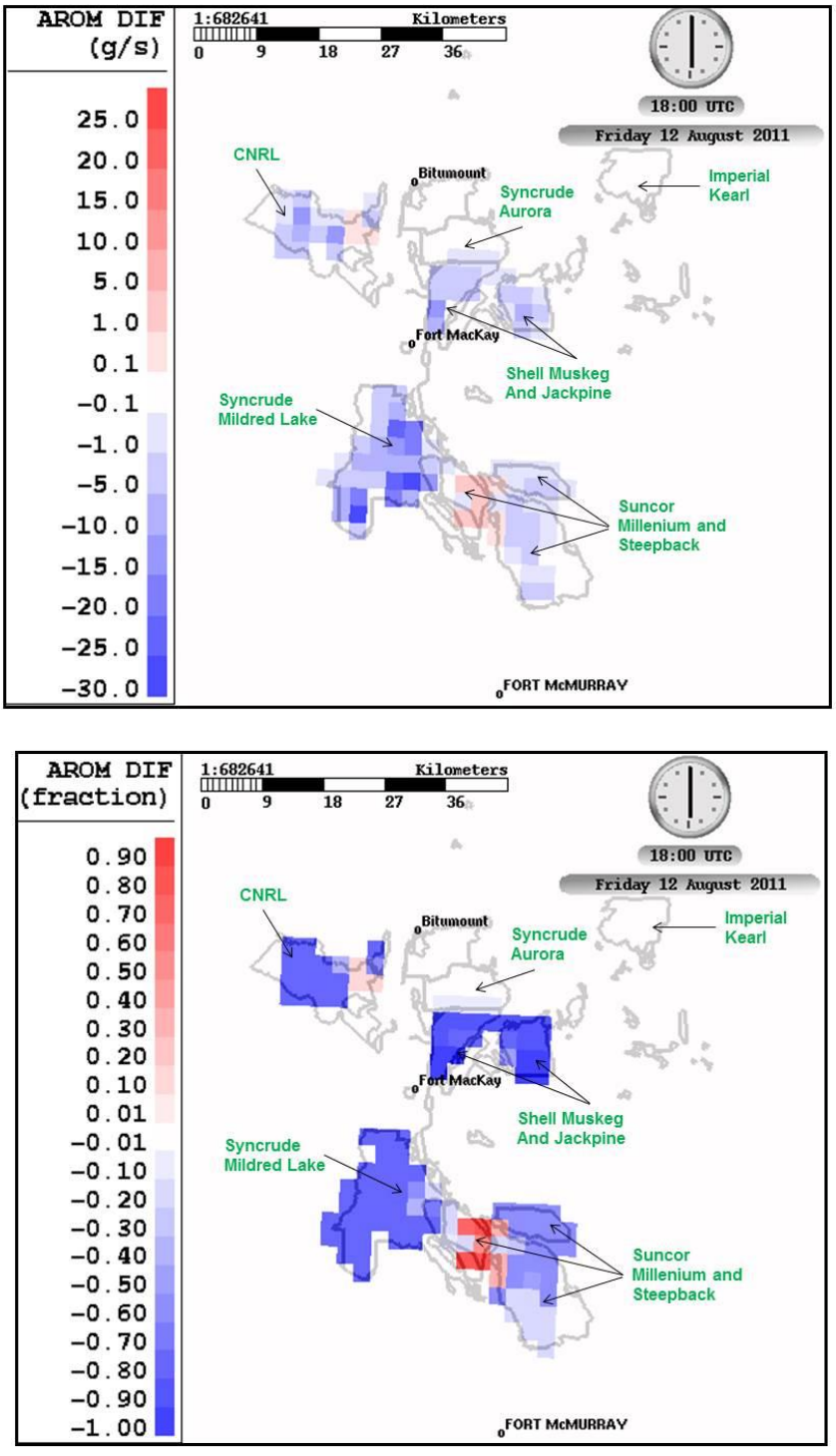

Figure S2. (a) Difference in AROM emissions (revised-base case) in units of grams/sec for a selected date and time; (b) relative difference calculated as (revised–base)/base. Large negative changes are noted over the Syncrude Mildred Lake facility.

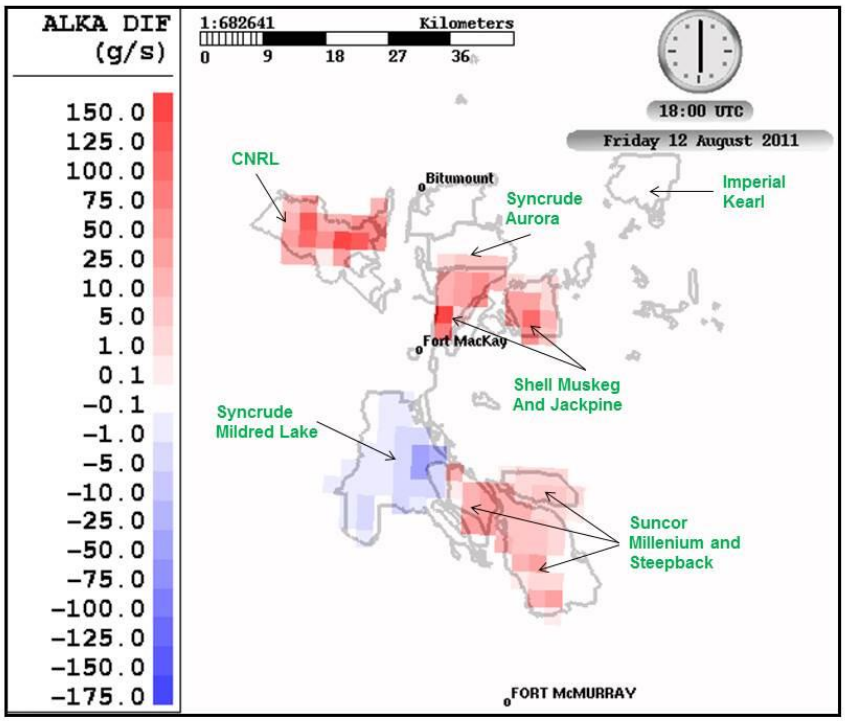

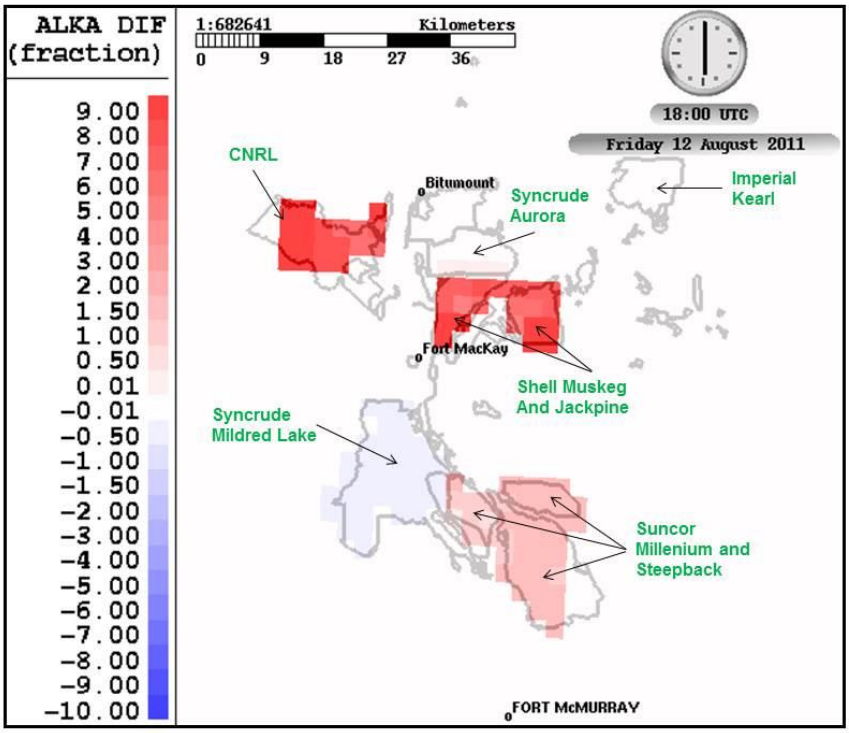

Figure S3. (a) Difference in lumped ALKA emissions (revised-base case) in units of grams/sec for each 2.5-km x 2.5-km grid cell; (b) relative difference calculated as (revised–base)/base.

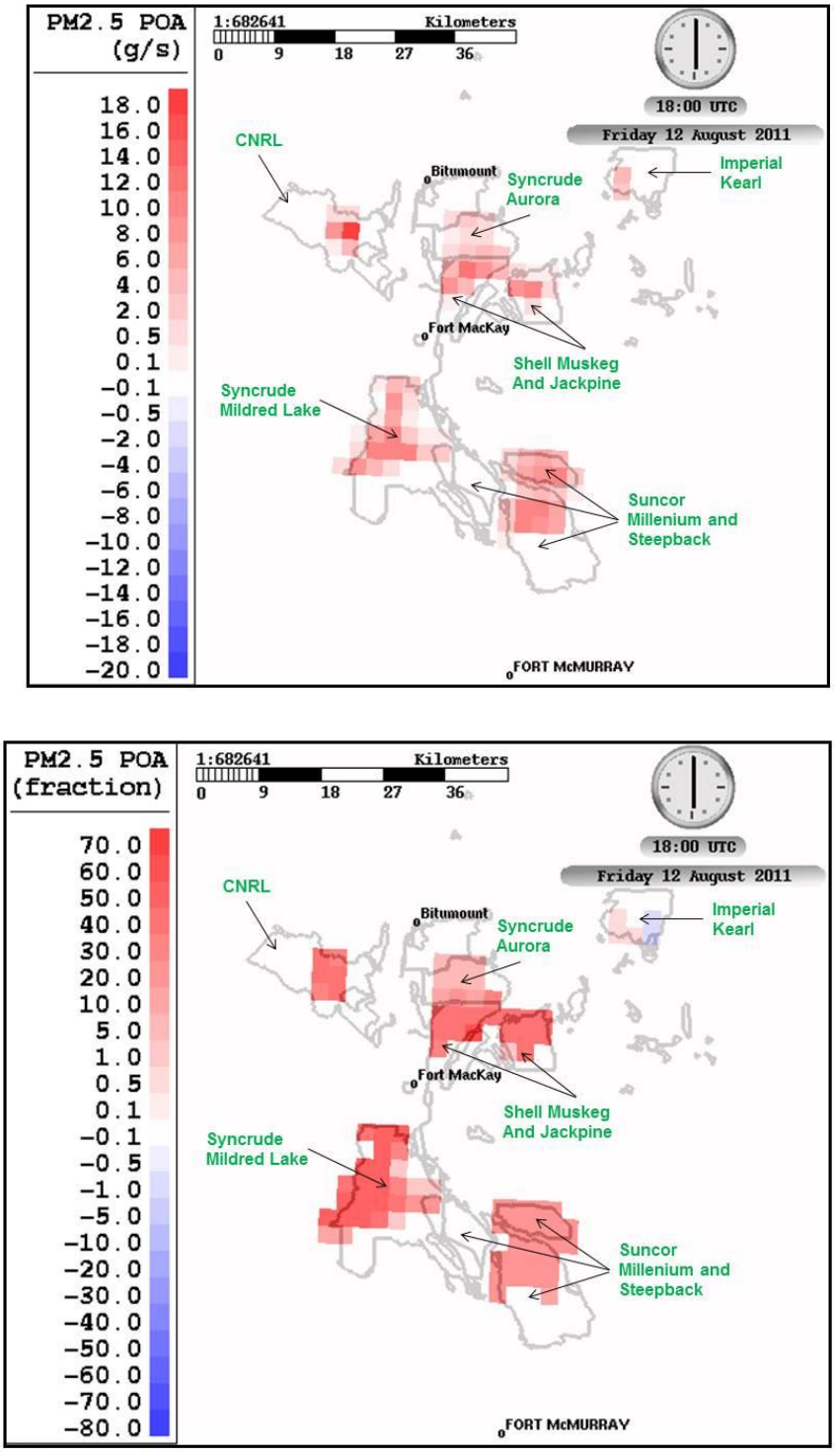

Figure S4. (a) Difference in primary organic aerosol (POA) emissions (revised-base case) in units of grams/sec for each 2.5-km x 2.5-km grid cell; (b) relative difference calculated as (revised–base)/base.

2. Case Study Analysis

We performed time series comparisons between the aircraft observations and the base case and sensitivity model data extracted along the individual flight tracks. The results are described below for the different organic species.

Mono-substituted Aromatics (TOLU)

Figure S5a shows the flight path for August 14, color-coded as a function of the difference between the modelled revised and base-case concentrations. The background is a satellite map image along with the GEM meteorological model wind barbs predicted for that day at 16 UTC. The largest differences in the simulated concentrations (1.8 ppbv) correspond to a location just downwind of the Syncrude Mildred Lake open-pit mine, as expected based on the emission difference map (Figure S1) and the southerly wind direction.

Figure S5b shows the time series for a segment of the August 14 flight corresponding to three flight boxes at different heights (green dotted line). The observations are plotted as open circles and the two lines represent the two model results. The model output with the revised VOC emissions clearly captures the main peak of the TOLU concentrations driven by TOLU emissions from the Syncrude Mildred Lake facility. The secondary peaks in the figure (a couple minutes apart from primary peaks) occur from the aircraft flying over the Suncor Millennium/Steepbank facility while on the east side of the flight box pattern. The direct flyover adds uncertainty to the model comparison, as it depends on predicting accurately the early-stage vertical mixing of the plume from the Suncor facility.

Figure S6 is a time-series segment for August 23 corresponding to a fly-over of the Syncrude Mildred Lake (earlier peak in time) and Suncor Millennium/Steepbank (later peak in time) facilities at a constant altitude of 300-magl. Winds were light on this day with variable swings in

direction. A double-peak pattern is observed in both the model and observations with a 1-min time shift needed to align the peaks. For this fly-over, the magnitude of the peaks is better represented with the revised emission model version. We note also that the one-minute lag time of the model peaks illustrates the difficulties in prediction of plume location at high resolution; this corresponds to an error in the forecast position of the plume of 6 km, or 2.4 of the model's grid-cells, given the aircraft's typical flight speed of 100 m s^{-1}. Small errors in wind direction, the potential for point sources located near grid-cell boundaries to effectively be re-located to the grid centroids, as well as directional errors in the forecasted winds, can contribute to these offsets between observed and simulated concentration peaks.

Multi-Substituted Aromatics (AROM)

Figure S7 shows the flight track for the August 23 survey flight, which flew over all the facilities. The background map shows model winds were light and variable on this afternoon. The flight track is color-coded as a function of the difference between AROM from the sensitivity-base case. Consistent with the emission changes, negative difference in ppbv were modelled over Syncrude, Shell, and CNRL and positive differences in ppbv over Suncor.

Figure S8a shows the time series for a segment of the August 23 survey flight over Syncrude Mildred Lake and Suncor Millennium/Steepbank. The largest maxima are for times over Syncrude (7:31Z) and, while both runs show an over-prediction in plumes, the sensitivity run predictions are closer to observations. Figure S8b is the time series for a short segment later in the flight for locations over the Syncrude (earlier peak in time) and Suncor (later peak in time) facilities. For the Suncor maximum, the sensitivity run with revised emissions has a better prediction for the magnitude of the mixing ratio change.

Figure S9a shows the flight track on September 3 over and around the Syncrude Mildred Lake facility. The flight path also included some turns over the Suncor Millennium/Steepbank facility. Similar to the August 23 flight, there are negative differences in the predicted AROM mixing ratio between the sensitivity and base runs over Syncrude and positive differences over Suncor. The decreases in mixing ratio are as large as 2 ppbv. Figure S9b is the time series for a segment of the September 3 flight. The observed mixing ratios are closer to the predictions from the revised-emissions model run compared to the base-case run.

Long Chain Alkanes (ALKA) Case Study Analysis

Figure S10a shows the differences between the two model predictions for ALKA at the observation canister sample locations, for the flight on August 26. On this day, winds were from the northeast and notably Fort McMurray (further to the south, not shown) had quite poor air quality. The largest differences in the modelled mixing ratios correspond to observation locations south of CNRL. Positive differences as large as 20 ppbv were simulated for some points. Figure S10b shows the time series for the observations, revised-emissions model results, and base-case model results for the August 26 box flight around the CNRL Horizon facility. A clear improvement in ALKA modelling is observed when using the revised emissions for the plume sampled downwind of the CNRL facility.

There were two other box flights around the CNRL Horizon facility. The flight on August 20 also showed an improvement in ALKA predictions when using the new emission data set. Winds were from the west on this day. The flight on Sept. 2 showed the opposite trend, with more of an over-prediction with the revised emissions. Winds were from the north on this day. The background ALKA on this flight was predicted to be higher for the sensitivity run; however,

the differences in mixing ratio between background and plume were over-predicted with the revised emissions and under-predicted with the base emissions.

The other facility that had large increases in ALKA emissions with the revised data was the Shell Muskeg/Jackpine facility (refer to Table 1 and Fig. S3). Flight 9 on August 21 was a box flight around the Shell facility. A detailed analysis of this flight showed that for the majority of the data points on this flight, the model run with the base-case emissions showed the best results, except for the three highest measured canister samples, where the model run with the revised emissions performed better. This likely reflects an uncertainty in the spatial allocation maps used to distribute the emissions with a higher fraction of emissions needed at the point specific locations.

Organic Aerosol

The focus of the flight on August 21 was a box pattern around the Shell Muskeg/Jackpine facility at different altitudes. The approach to this facility, however, also included an overpass of the Syncrude Mildred Lake facility. Figure S11ab illustrates the flight path color-coded as a function of POA difference (revised emissions – base case) and SOA difference (revised emissions –base case). The corresponding time series for OA observations, the revised emissions model run, and the base-case emissions model run OA predictions are shown in Figure S11c. There is a clear “hot spot” in POA difference in Figure S11a located over the Syncrude Mildred Lake facility. This hot spot corresponds to the first large maxima in the times series in Figure S11c (17:17 UTC). The observations at this time lie between the predictions from the two model simulations, though the overestimate of the revised emissions simulation is closer to the observations than the underestimate of the base-case emissions simulation. The aircraft then entered the box pattern at different altitudes around the Shell Muskeg/Jackpine facility, and each

successive pass around this facility intersected the observed plume on the north-east corner of the flight box (see hot-spot, Figure S11b); the model predicts that the increase in OA is largely due to SOA (as noted in Figure 7), and the revised-emissions simulation produces peak OA concentrations that are closer to the observations than the base-case emissions simulation. As is clear from Figure S11c, the base-case emissions simulation greatly underestimated the OA relative to observations. In examining the time series, it is also clear that both model simulations are under-estimating the background biogenic OA concentrations, by about 0.5 μg m^{-3}. The height of the peaks relative to background is closer to the sensitivity run peaks than the base-case run peaks.

Figure S12a shows the difference between revised-emissions and base-case model OA predictions for another case study on September 3, for southerly winds with a box flight over the Syncrude Mildred Lake facility. The flight started and ended with a horizontal zig-zag pattern with overpasses directly over the facility emissions sources. This corresponds to the initial spikes in the model in the time series shown in Figure S12b (8:30 p.m. UTC). Again, the observed height of the peaks lies between the model peak heights for the base-case and revised-emissions simulations. For this flight the background OA concentration is under-predicted by up to 2 μg/m^3 by the end of the flight. The background air has more measured oxygenated organic aerosol (OOA) (Liggio *et al*., 2016), with an aerosol mass spectra more reflective of laboratory monoterpene SOA (Han *et al*., 2017). During the box pattern, the peak heights in the observations more closely match the base model peaks. The PM_1 emission rates derived from the five box flights around Syncrude Mildred Lake did show more variability than for the other facilities. The average of five aircraft-derived PM_1 emission rates was used to revise the PM_1 emissions for Syncrude in the revised emissions data used by the model. Interestingly, the largest

observed OA value was measured in the spiral into the free troposphere near the end of the flight. There is no corresponding peak in the model at this time. The model peaks again only after the flight path has dropped into the boundary layer. Note that there was no corresponding increase in acetonitrile observed in the free troposphere so the source of the elevated OA is not likely from biomass burning, but may represent long-range transport from other sources.

The last case study is for the survey flight on August 23. Figure S13 shows the corresponding flight path color-coded by POA difference (revised - base case emissions; panel a) and SOA difference (revised – base-case emissions; panel b). From Figure S13a, we can again see the local maxima in POA difference between the runs over the Syncrude Mildred Lake facility. This corresponds to the peaks in time series at 5:50 p.m. UTC (Figure S13c). The observed peaks are closer in magnitude to the base-case model peaks at this time. The peak at 7:40 p.m. UTC corresponds to another time later in flight over the same location. The peak in SOA difference at 6:20 p.m. UTC is downwind of the CNRL Horizon facility (red points in Figure S13b). The observations show a more broadly spread-out peak at this time than is predicted by the model, perhaps indicating a greater degree of turbulence or wind variability in the observations than predicted by the model. Both modelled and observed meteorology had light wind speeds with a high degree of variability in direction on this day. The variability in the observed winds at the local Mildred Lake weather station was large on this afternoon with hourly-averaged wind directions of 40˚, 290˚, 180˚, 20˚, 40˚ from 12-16 UTC and wind speeds all less than 6 km/hr. These variable winds result in a more dispersed nature of the observed organic aerosol. The peak in observations at 6:25 p.m. UTC is represented well by the revised model. This corresponds to a location over Shell Muskeg/Jackpine (light blue points in Figure S13a). Note

that Figure S13c suggests that background OA levels once again seem to be under-estimated in both simulations.

References

Liggio, J., Li, S.-M., Hayden, K., Taha, Y.M., Stroud, C., Darlington, A., Drollette, B.D., Gordon, M., Lee, P., Liu, P., Leithead, A., Moussa, S.G., Wang, D., O'Brien, J., Mittermeier, R.L., Brook, J.R., Lu, G., Staebler, R.M., Han, Y., Tokarek, T.W., Osthoff, H.D., Makar, P.A., Zhang, J., Plata, D.L., and Gentner, D.R., Oil sands operations as a large source of secondary organic aerosols, Nature, 534 (7605), 91-94, **2016**.

Han, Y., Stroud, C.A., Liggio, J., and Li, S.-M., The effect of particle acidity on secondary organic aerosol formation from α-pinene photooxidation under atmospherically relevant conditions, Atmos. Chem. and Phys., 16 (21), 13929-13944, **2016**.

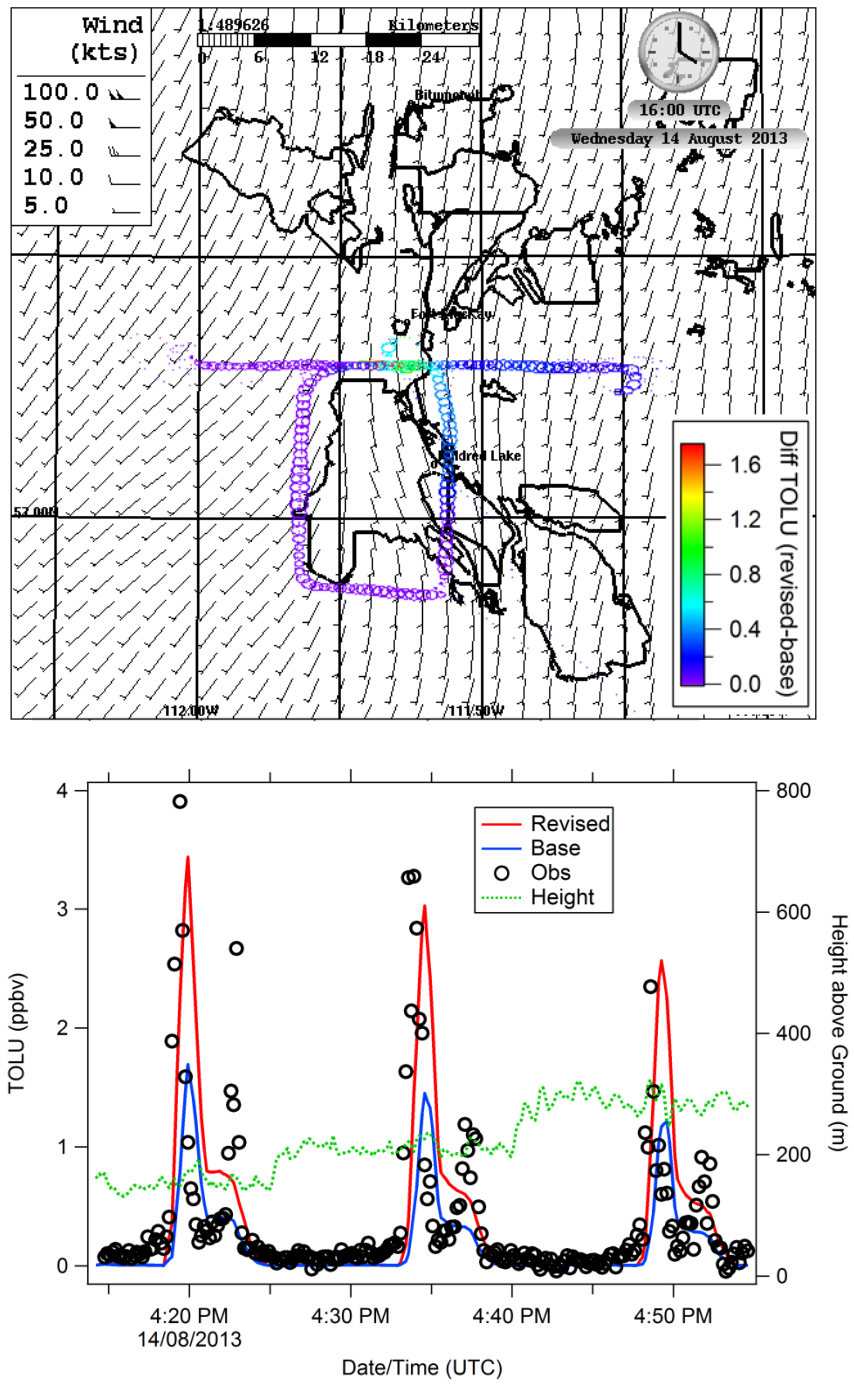

Figure S5ab. Flight track of the aircraft on Aug. 14, 2013 around the Syncrude Mildred Lake facility color-coded by the difference in TOLU volume mixing ratio (pptv) between the revised-emissions and the base-case simulations. The modelled wind barbs at the time of the maximum difference (16 UTC) are included in the background map. Panel b is the time series of observed and model-predicted TOLU volume mixing ratios for the flight on Aug. 14, 2013. The highest magnitude points correspond to a location north of the facility sampled at 3 different altitudes.

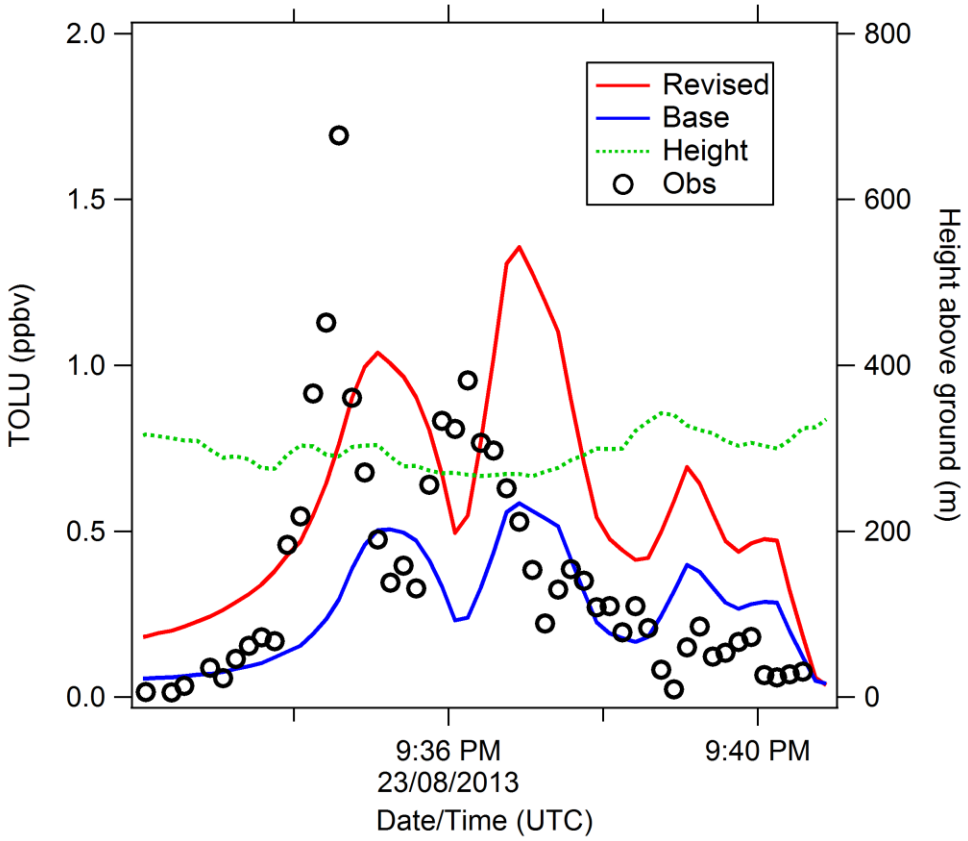

Figure S6. TOLU volume-mixing-ratio time series for a flight on Aug. 23, 2013 over the Suncor Millennium/Steepbank facility, just east of the Athabasca River, on a survey pattern.

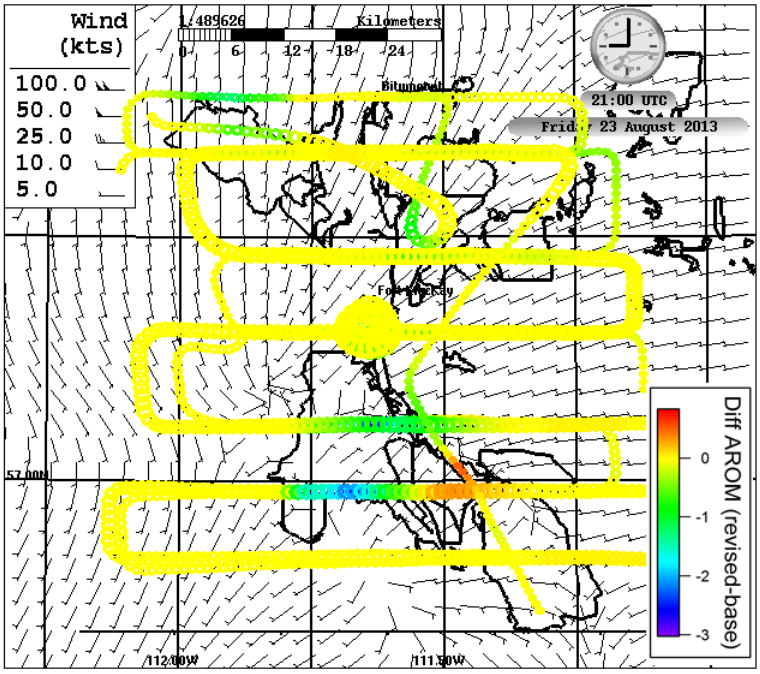

Figure S7. Flight track of the aircraft on Aug. 23, 2013 over all six OS surface mines color-coded by the difference in predicted AROM volume mixing ratio (pptv) between the revised-emissions and the base-case simulations. The modelled wind barbs at the time of the maximum difference (21 UTC) are included in the background map.

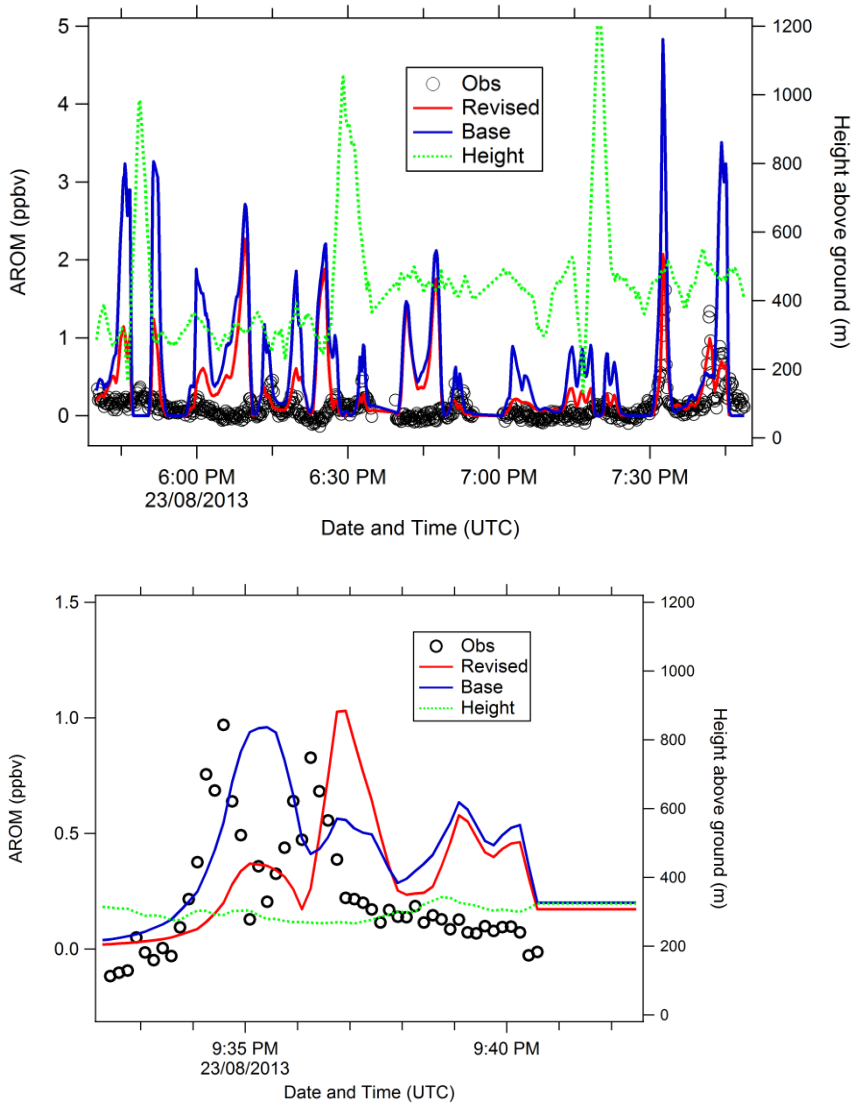

Figure S8ab. Time series of observed and model-predicted AROM volume mixing ratios for the Aug. 23 survey flight. The mixing-ratio peaks in panel A are over the Syncrude Mildred Lake facility (7:30-7:45 p.m. UTC). The 2nd peak in panel B is over the Suncor Millennium/Steepbank facility (9:37 p.m. UTC).

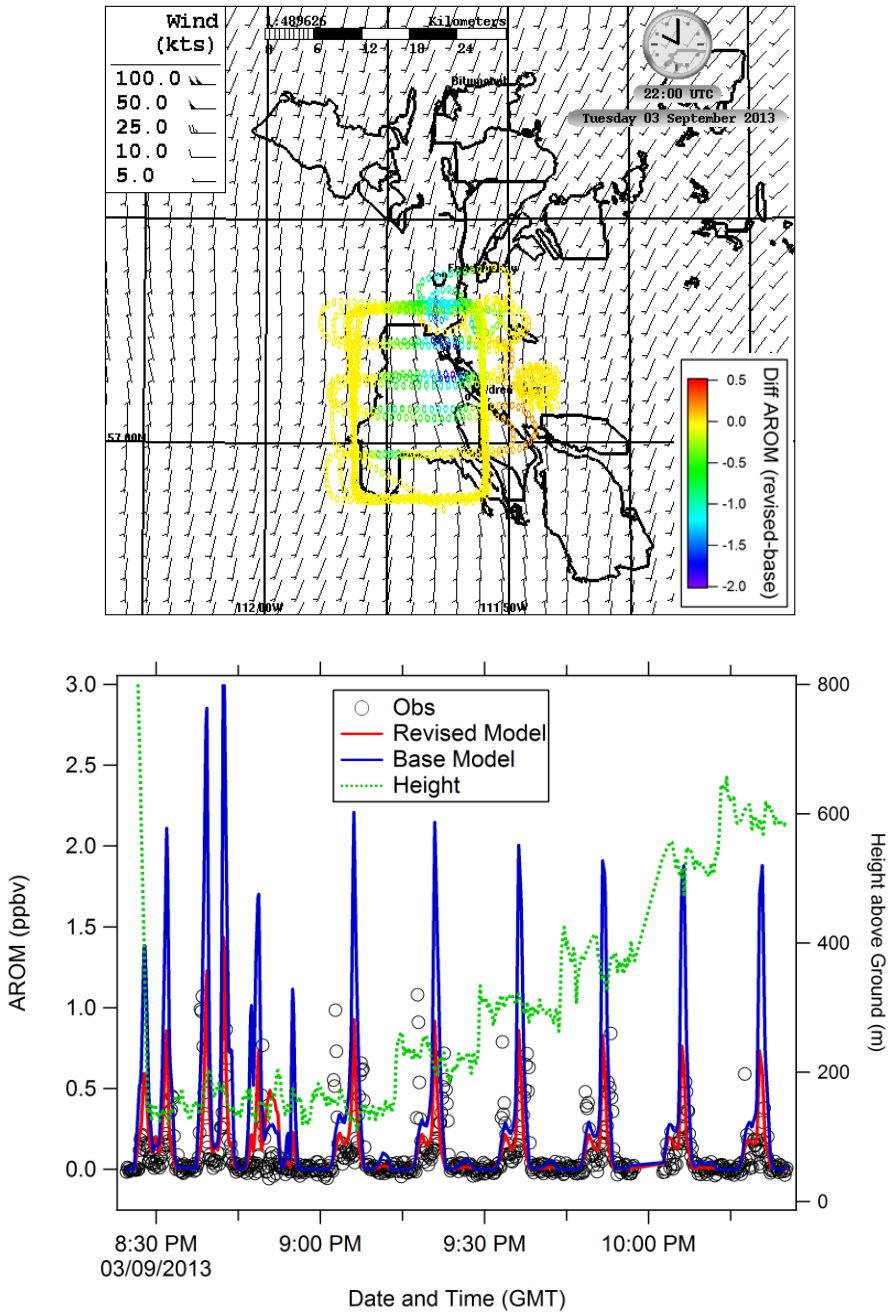

Figure S9ab. The top panel is the flight track of the aircraft on Sept. 3, 2013 over the Syncrude Mildred Lake facility color-coded by the difference in predicted AROM volume mixing ratio (pptv) between the revised-emissions and the base-case simulations. The modelled wind barbs at the time of the maximum difference (22 UTC) are included in the background map. The bottom panel is the AROM volume-mixing-ratio time series for the Sept. 3 flight around and over the Syncrude Mildred Lake facility.

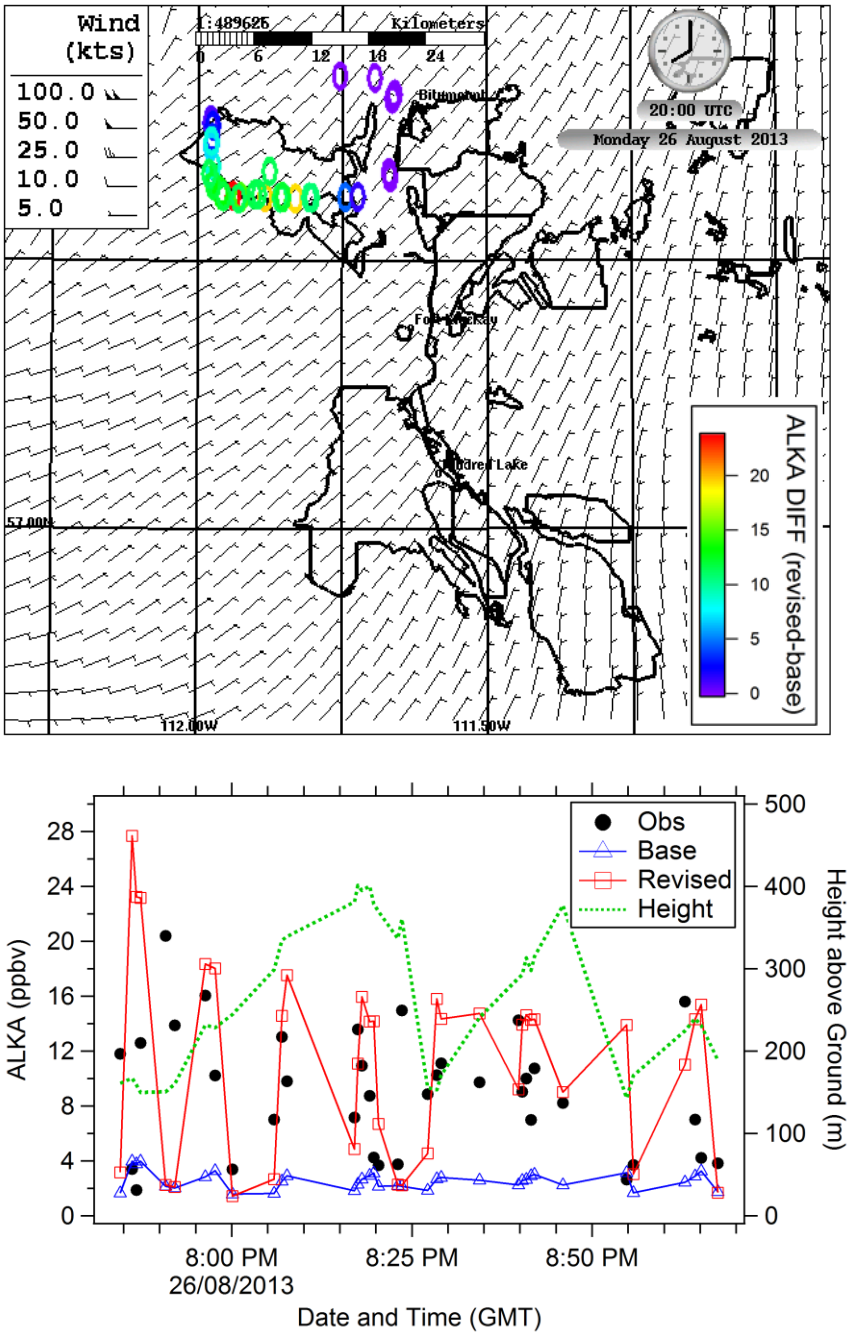

Figure S10ab. Flight track of the aircraft on Aug. 26, 2013 over the CNRL Horizon facility color-coded by the difference in predicted ALKA volume mixing ratio (pptv) between the revised-emissions and the base-case simulations. The modelled wind barbs at the time of the maximum difference (20 UTC) are included in the background map. The second panel is the ALKA volume-mixing-ratio time series for the Aug. 26 flight around the CNRL Horizon facility.

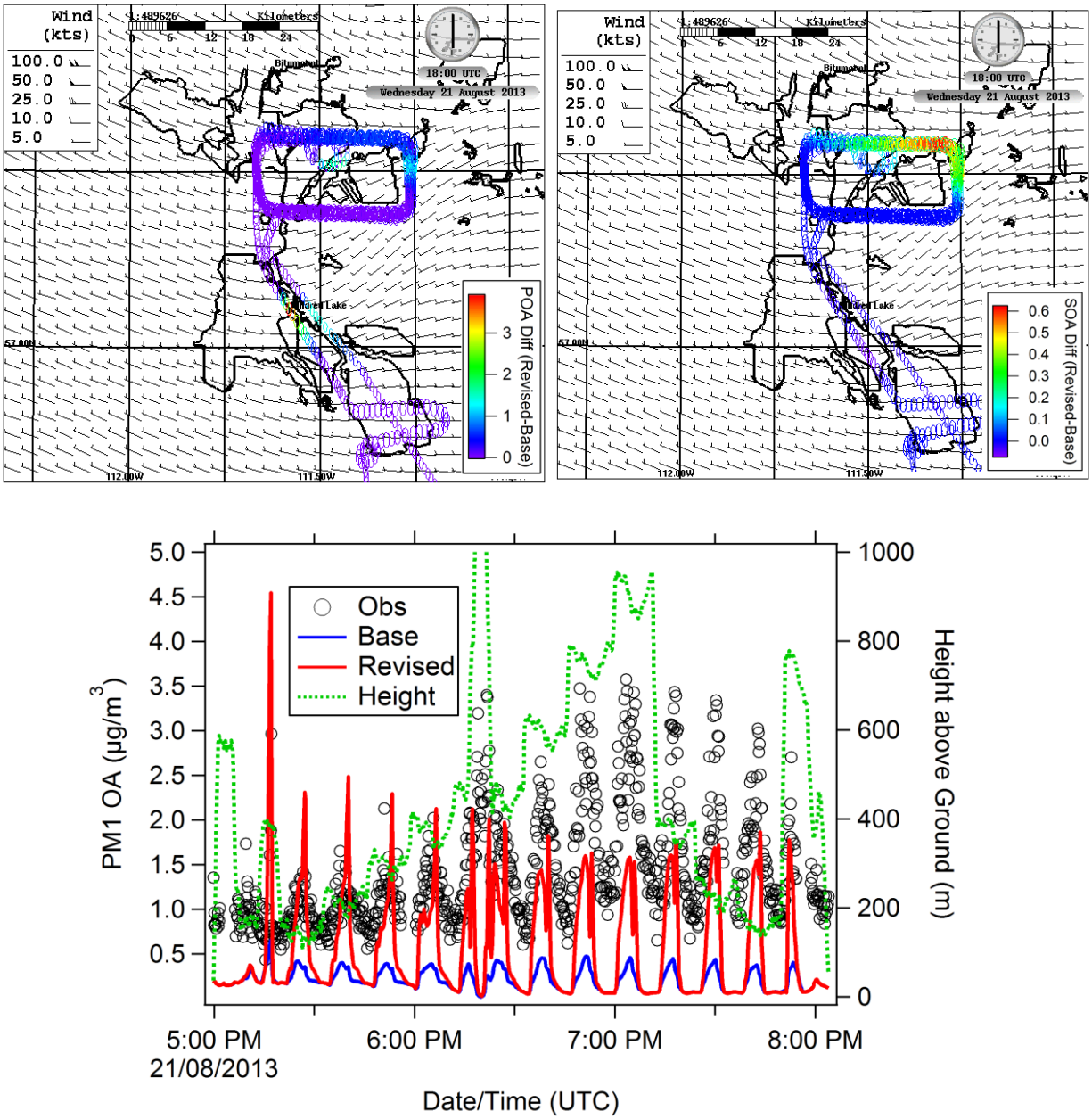

Figure S11abc. Flight track of the aircraft on Aug. 21, 2013 over the Shell Muskeg/Jackpine facility color-coded by the difference in predicted (a) POA concentration (µg/m^3) and (b) SOA concentration between the revised-emissions and the base-case-emissions simulations. The bottom panel is the time series for PM_1 organic aerosol concentration (µg/m^3) for the flight on August 21 crossing over the Syncrude Mildred Lake facility and then circling around the Shell Muskeg/Jackpine facility.

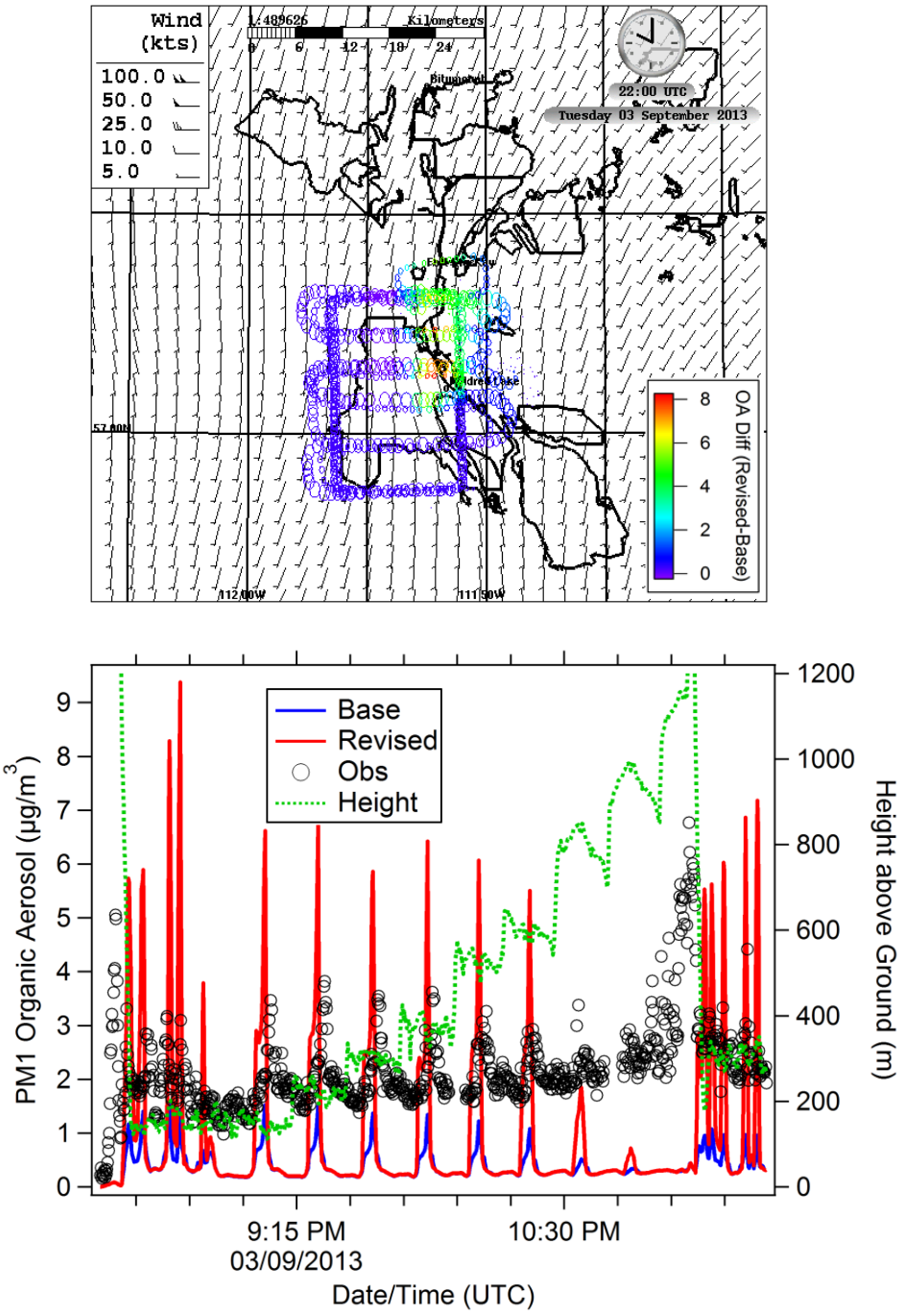

Figure S12ab. Flight track of the aircraft on Sept. 3, 2013 over the Syncrude Mildred Lake facility color-coded by the difference in predicted organic aerosol (OA) concentration (µg/m^3) between the revised-emissions and the base-case-emissions simulations. The bottom panel is the time series for PM_1 organic aerosol concentration (µg/m^3) for the Sept. 3 flight over and around the Syncrude Mildred Lake facility.

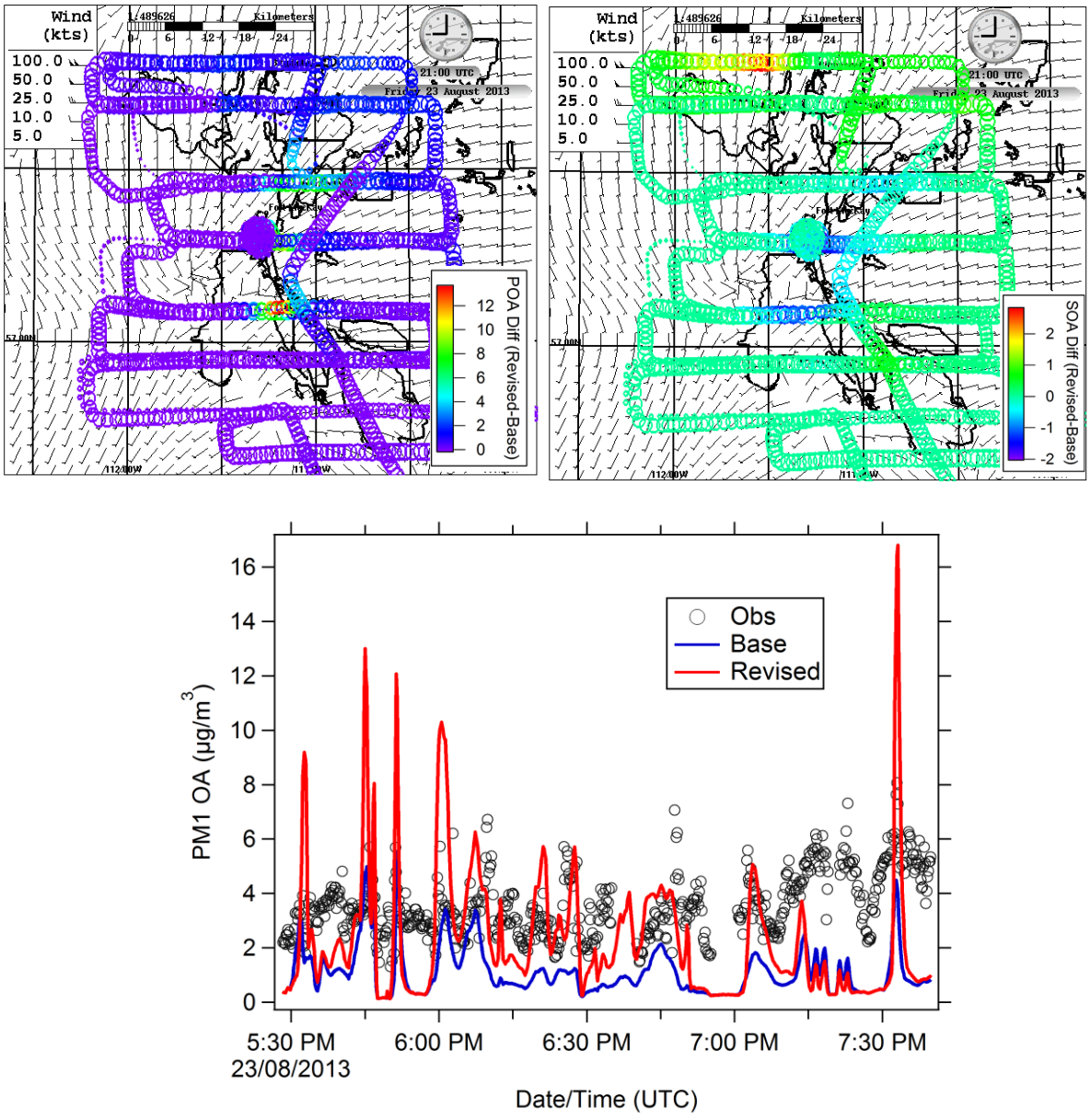

Figure S13abc. Flight track of the aircraft on Aug. 23, 2013 over all six OS surface mines color-coded by the difference in predicted (a) POA concentration (µg/m^3) and (b) SOA concentration between the revised-emissions and the base-case-emissions simulations. The bottom panel is the time series for PM_1 organic aerosol concentration (µg/m^3) for the Aug. 23 survey flight.